Journal for ImmunoTherapy of Cancer

BYON4228 is a pan-allelic antagonistic SIRPα antibody that potentiates destruction of antibody-opsonized tumor cells and lacks binding to SIRPγ on T cells

Mary J van Helden ,[1] Seline A Zwarthoff,[1] Roel J Arends,[1] Inge M J Reinieren-Beeren,[1] Marc C B C Paradé,[1] Lilian Driessen-Engels,[1] Karin de Laat-Arts,[1] Désirée Damming,[1] Ellen W H Santegoeds-Lenssen,[1] Daphne W J van Kuppeveld,[1] Imke Lodewijks,[1] Hugo Olsman,[2] Hanke L Matlung,[2] Katka Franke,[2] Ellen Mattaar-Hepp,[1] Marloes E M Stokman,[1] Benny de Wit,[1] Dirk H R F Glaudemans,[1] Daniëlle E J W van Wijk,[1] Lonnie Joosten-Stoffels,[1] Jan Schouten,[1] Paul J Boersema,[1] Monique van der Vleuten,[1] Jorien W H Sanderink,[1] Wendela A Kappers,[1] Diels van den Dobbelsteen,[1] Marco Timmers,[1] Ruud Ubink,[1] Gerard J A Rouwendal,[1] Gijs Verheijden,[1] Miranda M C van der Lee,[1] Wim H A Dokter,[1] Timo K van den Berg[1,2]

To cite: van Helden MJ, Zwarthoff SA, Arends RJ, *et al*. BYON4228 is a pan-allelic antagonistic SIRPα antibody that potentiates destruction of antibody-opsonized tumor cells and lacks binding to SIRPγ on T cells. *Journal for ImmunoTherapy of Cancer* 2023;**11**:e006567. doi:10.1136/jitc-2022-006567

► Additional supplemental material is published online only. To view, please visit the journal online (http://dx.doi.org/10.1136/jitc-2022-006567).

Accepted 26 March 2023

[1]Byondis BV, Nijmegen, Gelderland, The Netherlands
[2]Sanquin Research, Amsterdam, The Netherlands

Correspondence to
Dr Timo K van den Berg; Timo.vandenBerg@byondis.com

ABSTRACT

Background Preclinical studies have firmly established the CD47-signal-regulatory protein (SIRP)α axis as a myeloid immune checkpoint in cancer, and this is corroborated by available evidence from the first clinical studies with CD47 blockers. However, CD47 is ubiquitously expressed and mediates functional interactions with other ligands as well, and therefore targeting of the primarily myeloid cell-restricted inhibitory immunoreceptor SIRPα may represent a better strategy.

Method We generated BYON4228, a novel SIRPα-directed antibody. An extensive preclinical characterization was performed, including direct comparisons to previously reported anti-SIRPα antibodies.

Results BYON4228 is an antibody directed against SIRPα that recognizes both allelic variants of SIRPα in the human population, thereby maximizing its potential clinical applicability. Notably, BYON4228 does not recognize the closely related T-cell expressed SIRPγ that mediates interactions with CD47 as well, which are known to be instrumental in T-cell extravasation and activation. BYON4228 binds to the N-terminal Ig-like domain of SIRPα and its epitope largely overlaps with the CD47-binding site. BYON4228 blocks binding of CD47 to SIRPα and inhibits signaling through the CD47-SIRPα axis. Functional studies show that BYON4228 potentiates macrophage-mediated and neutrophil-mediated killing of hematologic and solid cancer cells in vitro in the presence of a variety of tumor-targeting antibodies, including trastuzumab, rituximab, daratumumab and cetuximab. The silenced Fc region of BYON4228 precludes immune cell-mediated elimination of SIRPα-positive myeloid cells, implying anticipated preservation of myeloid immune effector cells in patients. The unique profile of BYON4228 clearly distinguishes it from previously reported antibodies representative of agents in clinical development, which either lack recognition of one of the two SIRPα polymorphic variants (HEFLB), or cross-react with SIRPγ and inhibit CD47-SIRPγ interactions (SIRPAB-11-K322A, 1H9), and/or have functional Fc regions thereby displaying myeloid cell depletion activity (SIRPAB-11-K322A). In vivo, BYON4228 increases the antitumor activity of rituximab in a B-cell Raji xenograft model in human $SIRP\alpha_{BIT}$ transgenic mice. Finally, BYON4228 shows a favorable safety profile in cynomolgus monkeys.

Conclusions Collectively, this defines BYON4228 as a preclinically highly differentiating pan-allelic SIRPα

WHAT IS ALREADY KNOWN ON THIS TOPIC

⇒ The CD47-signal-regulatory protein (SIRP)α axis functions as a myeloid immune checkpoint and agents targeting this pathway have shown encouraging results in early clinical trials in patients with cancer.

WHAT THIS STUDY ADDS

⇒ We report the generation and preclinical characterization of a novel SIRPα blocking antibody, BYON4228. Side-by-side comparisons with other previously described SIRPα blocking antibodies show that BYON4228 has a unique and favorable preclinical profile.

HOW THIS STUDY MIGHT AFFECT RESEARCH, PRACTICE OR POLICY

⇒ BYON4228 has the potential to become a best-in-class CD47-SIRPα antagonist.

antibody without T-cell SIRPγ recognition that promotes the destruction of antibody-opsonized cancer cells. Clinical studies are planned to start in 2023.

BACKGROUND

Antibodies against tumor-associated antigens (anti-TAAs) play a prominent role in the treatment of a broad range of solid and hematologic cancers.[1] Some of the most commonly used examples of anti-TAAs include trastuzumab directed against Her2 (over)expressed on breast and other types of cancer cells, cetuximab directed against the epidermal growth factor receptor (EGFR) on various carcinoma cells, rituximab directed against CD20 expressed on malignant B cells, and daratumumab directed against CD38 on multiple myeloma cells. Generally, anti-TAAs act by a combination of target-related direct and immune-mediated mechanisms. The immune-mediated mechanisms include complement-dependent cytotoxicity (CDC), effector cell-mediated antibody-dependent cellular cytotoxicity (ADCC) performed by natural killer (NK) cells and granulocytes, and antibody-dependent cellular phagocytosis (ADCP) exerted by macrophages.[2–6] Furthermore, anti-TAAs can also effectively trigger adaptive T cell-mediated immunity by facilitating cross-presentation of tumor antigens to cytotoxic T lymphocytes.[7] All these immune effector cell responses are triggered by the Fc regions of anti-TAAs that ligate activating Fc receptors and thereby initiate intracellular signaling and (direct or indirect) downstream tumor cell elimination. Despite this multitude of mechanisms, there remains a pertinent need to improve anti-TAAs clinical efficacy.

The CD47-signal-regulatory protein (SIRP)α axis has been firmly established as a myeloid immune checkpoint in preclinical and in early stage clinical studies.[8–12] SIRPα is a typical inhibitory immunoreceptor primarily expressed on myeloid cells, including monocytes, macrophages, granulocytes and dendritic cell subsets.[13–16] Two polymorphic variants are present in the human population, named $SIRP\alpha_{BIT}$ (also known as V1) and $SIRP\alpha_{1}$ (also known as V2). SIRPα is the only inhibitory member of a multigene receptor family with the closest homologs in humans and other primates being SIRPβ1v1, SIRPβ1v2 and SIRPγ.[17] CD47, also known as integrin-associated protein, is the cellular ligand for SIRPα and SIRPγ, but not for the two SIRPβ1 receptors.[18–22] CD47 is broadly expressed on most if not all cells in the body and is often found to be overexpressed on cancer cells.[9 10] Cellular CD47 binding to SIRPα triggers inhibitory intracellular signaling via immunoreceptor tyrosine-based inhibitory motifs in the SIRPα cytoplasmic tail involving the recruitment and activation of the tyrosine phosphatases SH2 domain-containing protein-tyrosine phosphatases (SHP)-1 and/or SHP-2, which restricts myeloid effector function.[13 15 16 23–26] Consequently, blockade of CD47-SIRPα signaling can promote macrophage-mediated and neutrophil-mediated tumor cell destruction in the presence of cancer-opsonizing antibodies, or other pro-phagocytic signals.[9–11 27–30] In addition, there is accumulating evidence that disruption of the CD47-SIRPα signaling axis promotes adaptive anticancer immunity[31 32] in combination with programmed cell death protein-1 (PD-1)/programmed death ligand-1 checkpoint inhibitors,[33 34] or other approaches such as radiotherapy that can also trigger antitumor immunity.[35]

Around 35 therapeutics directed towards the CD47-SIRPα axis have entered clinical trials in recent years.[36–38] The first clinical studies were performed with CD47-targeting agents, used as single agents or in combination with anti-TAAs or anti-PD-1, and have shown limited toxicity and promising initial efficacy.[36 37 39–41] However, conceptually there appear to be several disadvantages of targeting CD47 per se. First, CD47 is not specific for tumor cells. In fact, CD47 is widely distributed, therefore forming a large 'antigen sink' requiring high doses of drug for saturation. Furthermore, many CD47-targeting agents have Fc tails with normal effector functions, including Fc receptor binding, and this may opsonize normal cells and cause toxicity, for instance, by promoting the immune-mediated destruction of such healthy cells. Indeed, anemia and thrombocytopenia are common side effects of CD47 targeting agents with functional Fc regions, often requiring red blood cell transfusion, even though a low-dose priming strategy has been adopted to mitigate this to some extend.[36 39] Finally, CD47 does not only bind SIRPα but it also mediates functional interactions with integrins,[22 42] vascular endothelial growth factor-2[43] thrombospondin-1[44] and SIRPγ,[45] and these may be affected by CD47-targeting agents too. The most notable of these other CD47 ligands is SIRPγ, a close homolog of SIRPα present only in primates, which is expressed on T cells and activated NK cells.[45] CD47-SIRPγ interactions are pivotal for T-cell extravasation and activation and their disruption might therefore curtail durable antitumor immunity.[34 46–48] Thus, targeting of CD47 may not be the most optimal way to selectively antagonize CD47-SIRPα interactions and therefore therapeutic targeting of the myeloid cell-restricted SIRPα may represent a better strategy.

Currently, four therapeutic SIRPα-targeting antibodies have entered clinical development in cancer indications: BI 765063 (NCT03990233, NCT04653142, NCT05249426, NCT05446129), BI 770371 (NCT05327946; no details on the antibody nor its properties have been disclosed yet), BMS-986351 (NCT03783403, NCT05168202), and GS-0189 (NCT04502706) (also see table 1). However, most of the anti-SIRPα antibodies HEFLB, 1H9, and SIRPAB-11, which in all probability are representative for three of the clinical stage SIRPα antibodies (see table 1), have been reported to lack binding to both polymorphic SIRPα variants that are present in the human population, or they also recognize the related SIRPγ.[29 34 49–54]

Here we report the preclinical characterization of BYON4228 and a direct in vitro comparison with the three anti-SIRPα antibodies HEFLB, 1H9 and SIRPAB-11.

Table 1 Properties of anti-SIRPα antibodies used for in vitro comparisons

mAb	Source of sequences	Fc tail	Names of corresponding agent in clinical trials*
HEFLB	WO 2017/178653	IgG4-S228P/L445P	BI-765063 OSE-172
SIRPAB-11-K322A	WO 2020/068752	IgG1-K322A	BMS-986351 Anzurstobart CC-95251
1H9	WO 2019/023347	IgG1-N297A	GS-0189 FSI-189

*Based on data provided in Gauttier *et al*,[34] WO 2017/178653[54] and WO 2019/175218,[70] HEFLB most likely corresponds to BI-765063/OSE-172; based on identity of amino acid sequences in the publication of the International Non-proprietary Name (WHO Drug Information Vol 36 No 2 2022, p319) and WO 2020/068752,[58] SIRPAB-11-K322A corresponds to anzurstobart/BMS-986351/CC-95251; based on data provided in Liu *et al*[49] and a Forty Seven Inc. Corporate presentation of 2020,[71] 1H9 most likely corresponds to GS-0189/FSI-189.
mAb, monoclonal antibody ; SIRP, signal-regulatory protein.

BYON4228 is a pan-allelic SIRPα antibody that lacks binding to SIRPγ present on T cells. BYON4228 binds to a region overlapping with the CD47 binding site on SIRPα, thereby preventing binding of CD47 to SIRPα and blocking inhibitory signaling. BYON4228 potentiates killing and phagocytosis by human neutrophils and macrophages, respectively, of hematologic and solid tumor cells opsonized with various anti-TAAs. Silencing of the BYON4228 Fc tail prevents unwanted destruction of SIRPα-positive myeloid cells. In a human $SIRP\alpha_{BIT}$ transgenic mouse model, BYON4228 promotes rituximab-dependent elimination of Raji cells. Finally, intravenous single dose infusion of up to 100 mg/kg and repeated dose infusion of up to 30 mg/kg BYON4228 to cynomolgus monkeys is well tolerated. These data support further development of BYON4228 in clinical trials.

METHODS

Detailed methods can be found in the online supplemental materials.

BYON4228 antibody development and humanization

BYON4228 was generated by immunization of rabbits with the extracellular domains (ECDs) of SIRPα allelic variants, sequencing PCR products from selected B cells and humanization.

HEFLB, SIRPAB-11-K322A, 1H9 antibody sequences

The sources of the antibody amino acid sequences of HEFLB, SIRPAB-11-K322A (referred as SIRPAB-11 in this paper) and 1H9 (the latter generated as a G1m17,1 allotype) (also see online supplemental materials) and their presumed equivalents in clinical trials are shown in table 1.

Anti-TAAs

The following anti-TAAs were used: rituximab (MabThera, Roche), daratumumab (DARZALEX, Janssen Biologics), panitumumab (Vectibix, Amgen), cetuximab (Erbitux, Merck) and trastuzumab (Herceptin, Roche).

Cellular binding to SIRP-expressing Expi Chinese hamster ovary-S cells and primary granulocytes

Transiently transfected Expi Chinese hamster ovary-S (ExpiCHO-S) cells were first incubated for 30 min with primary antibodies and then with AF647-conjugated or R-phycoerythrin (PE)-conjugated anti-human IgG antibodies. Median fluorescent intensities were determined by flow cytometry (FACSympony or FACSVerse, BD Bioscience) or relative fluorescence units were determined (EnVision, PerkinElmer).

CD47-bead and mAb binding to U937 cells and primary cells

Peripheral blood mononuclear cells (PBMCs) or U937 cells were stained with Alexa Fluor 647-labeled antibodies and then incubated with CD47-Fc-coated fluorescent beads plus anti-CD3 allophycocyanin-H7 and anti-CD14 PerCp-Cy5.5. After 30 min and washing, the cells were analyzed using flow cytometry (FACSympony or FACSVerse, BD Bioscience).

ADCP and ADCC

ADCP was performed using confocal microscopy (CD20-positive target cells) or live cell imaging (CD20-negative target cells). Monocytes were differentiated to macrophages with macrophage colony-stimulating factor) for 7 days. Fluorescently labeled or pHrodo-labeled target cells and antibodies were added for 3–8 hours at 37°C in the presence of 100 µg/mL intra-venous immunoglobulins (IVIg). For confocal ADCP, the cells were counterstained with anti-CD19-PE and Hoechst 33342 to determine phagocytosis (ImageXpress, Molecular Devices). For live cell imaging based ADCP, images were taken every 30 or 60 min using a real-time fluorescence imager (IncuCyte, Sartorius). For ADCC, human neutrophils were isolated, activated for 30 min with 10 ng/mL granulocyte-macrophage colony-stimulating factor (GM-CSF), incubated for 4 or 20 hours with 100 µCi Cr-51 labeled target cells (effector:target ratio of 50:1), and killing was determined by analyzing the supernatant in

a scintillation counter (MicroBeta[2] Microplate Counter, PerkinElmer).

Raji xenograft in human SIRPα$_{BIT}$-severe combined immunodeficiency transgenic mice

Tumors were induced by subcutaneous (SC) injection of 2×10^7 Raji cells into the flank of female human SIRPα$_{BIT}$-severe combined immunodeficiency (scid) animals. BYON4228 was administered intraperitoneal (IP) three times a week for 4 weeks at a dose of 5 mg/kg. Rituximab was administered at 1 mg/kg IP.

Graphical representation, curve fitting and statistical analysis

Dose-response curves were fitted by non-linear regression with a variable slope (four parameters) in GraphPad Prism 9. EC_{50} or IC_{50} values were calculated in GraphPad Prism as the concentration that gives a response halfway between bottom and top of the curve. Statistical testing was performed in GraphPad Prism 9 as indicated in the figure legends. For functional assays (ADCC, ADCP), statistical analysis was performed on the 'fold enhancement' graphs. Since no values could be calculated for non-/poor-responsive donors, statistical tests were not performed on EC_{50} and IC_{50} summarizing graphs or figures 3B and 4C.

RESULTS

BYON4228 is a high affinity pan-allelic SIRPα antibody

We aimed to generate a blocking antibody against the inhibitory receptor SIRPα that binds to both the SIRPα$_{BIT}$ and SIRPα$_1$ polymorphic variants, but lacks binding to SIRPγ on human T cells. The blocking antibody should disrupt the binding of CD47 to SIRPα and inhibit CD47-induced SIRPα signaling. Rabbits were immunized with a mixture of proteins representing the ECDs of both SIRPα allelic variants and cynomolgus SIRPα. B cells from these rabbits were screened for antibody production levels, antigen binding and blocking to select B-cell clones producing antibodies that met our criteria. The variable domains of these B-cell clones were used to produce chimeric antibodies with hIgG1 backbone to allow further selection rounds. Ultimately, we selected BYON4228, a humanized antibody that met all our pre-set criteria, and compared it to three SIRPα antibodies that are considered to be representative of three clinical stage SIRPα antibodies (table 1). BYON4228 bound to both SIRPα$_{BIT}$ and SIRPα$_1$ with high affinity (table 2, figure 1A,B). Clearly, this pan-allelic characteristic was not a common property of all other SIRPα-antibodies tested. In particular we found, in line with earlier publications,[51 55] that the SIRPα antibody HEFLB did not display binding to SIRPα$_1$ (figure 1A,B). All four anti-SIRPα monoclonal antibodies (mAbs) tested (ie, BYON4228, HEFLB, SIRPAB-11 and 1H9) showed binding to SIRPβ1v1 and SIRPβ1v2, although with variable EC_{50} values (figure 1A,B). In line with its binding specificity, BYON4228 potently bound to primary SIRPα-expressing immune cells irrespective of their SIRPα-genotype (figure 1C,D). Overall, these results show that BYON4228 is a high-affinity pan-allelic SIRPα antibody that binds its native antigen on myeloid cells.

Table 2 Overview of observed affinities of BYON4228

Ligand for BYON4228	Observed affinities (K_D-obs)	
	Antigen on surface set-up	Antibody on surface set-up
Human SIRPα$_1$ ECD	<0.010 nM	1.94 nM
Human SIRPα$_{BIT}$ ECD	0.123 nM	24.3 nM
Human SIRPβ1v1 ECD	0.040 nM	8.66 nM*
Human SIRPβ1v2 ECD	3.16 nM	>100 nM†

*Kinetic parameters were estimated using a C1 chip instead of a CM5 chip (used for the other measurements).
†Fast on, fast off binding, no kinetic parameters could be estimated.
ECD, extracellular domain; NB, no binding; SIRP, signal-regulatory protein .

BYON4228 binds to a conserved epitope on the CD47-binding domain of SIRPα and blocks signaling

The extracellular region of SIRPα consists of three immunoglobulin superfamily (IgSF) domains and the first N-terminal V-set IgSF domain mediates binding to CD47.[21] To identify the domain to which BYON4228 binds, we took advantage of the finding that BYON4228 lacks binding to SIRPγ (online supplemental figure S1A, table 3) and generated various chimeric SIRPα-SIRPγ domain swapped proteins. Binding of BYON4228 to these chimeric proteins could only be detected when domain 1 was derived from SIRPα, but not from SIRPγ. The origin of domain 2 and 3 was irrelevant for BYON4228 binding, showing that SIRPα domain 1 is both essential as well as sufficient for BYON4228 binding. Therefore, the BYON4228 epitope is present within this domain (online supplemental figure S1A). To define in more detail the epitope of BYON4228, we employed hydrogen deuterium exchange mass spectrometry technology. This method relies on the hydrogen to deuterium exchange, which occurs when molecules are incubated in heavy water. When a protein is complexed with an antibody, the deuterium uptake is hampered in the binding region, which can be measured using mass spectrometry. Using this method, BYON4228 binding signals were detected in the regions between residues 26–40, 50–62 and 95–103 (online supplemental figure S1B) of both SIRPα$_{BIT}$ and SIRPα$_1$. For visualization, the epitope was projected onto the N-terminal Ig-like CD47-binding domain of SIRPα$_{BIT}$ and SIRPα$_1$, previously resolved by X-ray crystallography.[21 56] A large overlap with the CD47 binding site was noted (figure 2). The binding site covered almost exclusively non-polymorphic amino acid residues (online supplemental figure S1C), in line with the potent binding of BYON4228 to both SIRPα$_{BIT}$ and SIRPα$_1$. In conclusion, these results show that the BYON4228 epitope maps

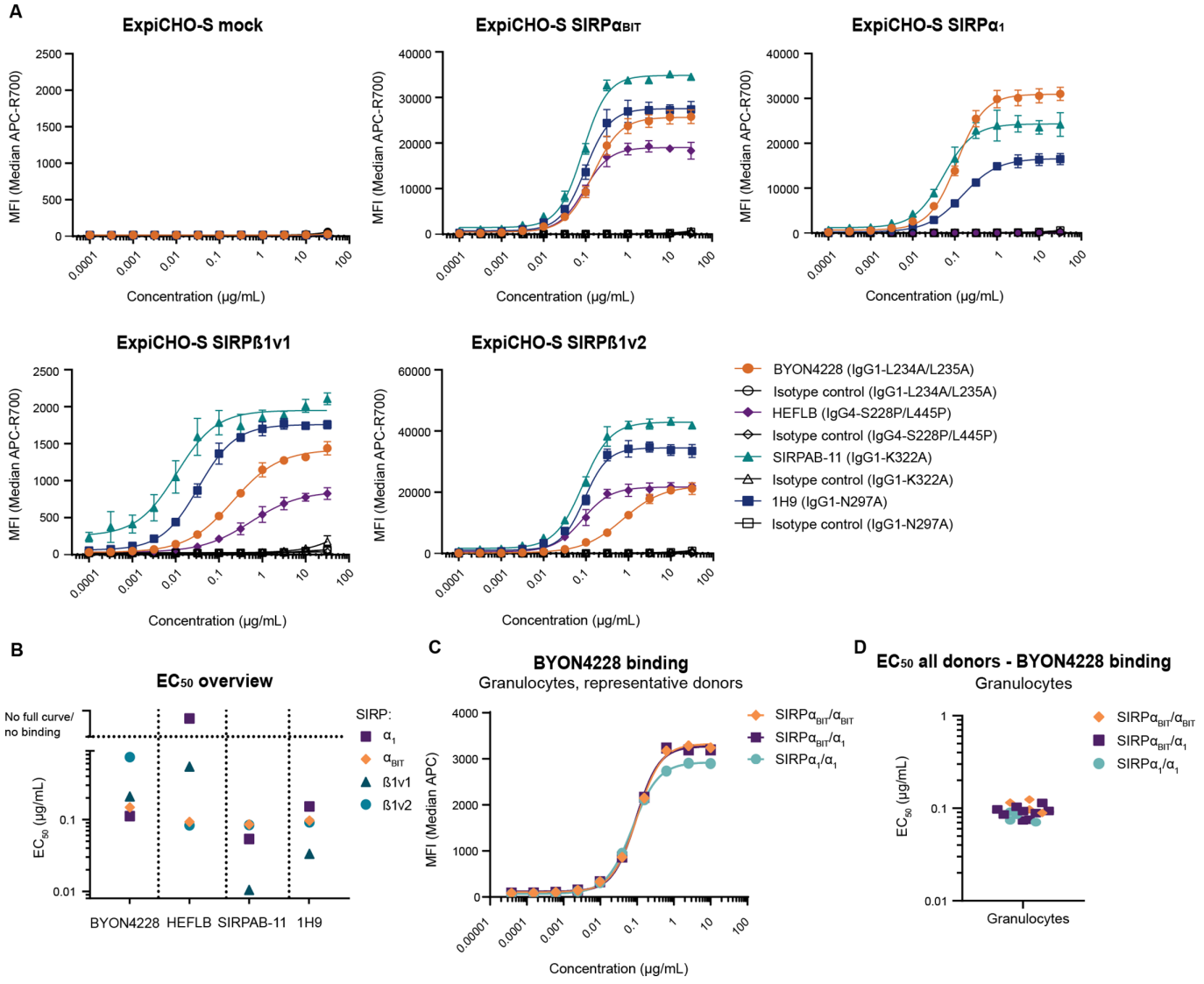

Figure 1 BYON4228 is a high affinity pan-allelic SIRPα binding antibody. (A,B) Binding of indicated SIRPα antibodies and respective isotype control antibodies to ExpiCHO-S cells that transiently expressed indicated SIRP molecules or were mock transfected. (A) Average median fluorescence intensity (MFI) ±SD of N=3 independent experiments are depicted. (B) Overview of the geomean EC_{50} values per antibody. (C,D) Cellular binding of BYON4228 (IgG1-L234A/L235A) to gated erythrocyte-lysed granulocytes from representative healthy donors with indicated SIRPα genotypes (C) and the EC_{50} summary of BYON4228 for all donors (N=17) (D). APC, allophycocyanin; ExpiCHO-S, Expi Chinese hamster ovary-S; SIRP, signal-regulatory protein.

to the CD47 binding site on the membrane distal domain of SIRPα.

To test the ability of BYON4228 to disrupt the interaction between SIRPα and CD47, PBMCs were incubated with fluorescent beads coated with human CD47. The CD47-beads bound to SIRPα-expressing monocytes and BYON4228 was able to inhibit such binding in a dose-dependent manner, irrespective of the SIRPα-genotype (figure 3A,B). While all four tested anti-SIRPα antibodies showed binding to primary monocytes of all SIRPα-genotypes, HEFLB was unable to inhibit CD47 binding to monocytes of $SIRP\alpha_1/\alpha_1$ donors and inhibited CD47-bead binding to monocytes of $SIRP\alpha_{BIT}/\alpha_1$ donors with limited efficacy (figure 3A,B). The binding

Table 3 Observed affinities of BYON4228 for binding to human SIRPγ

	Observed affinities (K_D-obs)	
Ligand for BYON4228	**Antigen on surface set-up**	**Antibody on surface set-up**
Human SIRPγ ECD	NB	*

*Dose-dependent very low binding responses were observed; no K_D could be estimated.
ECD, extracellular domain; NB, no binding; SIRP, signal-regulatory protein.

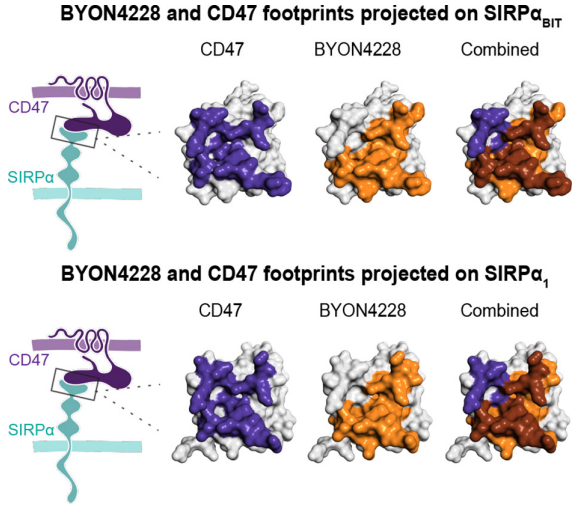

Figure 2 BYON4228 binds to the CD47-binding domain of SIRPα. (A) The BYON4228 epitope was mapped using HDX-MS. Projection of the CD47 binding site[21 56] (purple, left), BYON4228 HDX-MS mapped epitope (orange, middle) and overlap (brown, right) onto the N-terminal Ig-like CD47-binding domain of SIRPα$_{BIT}$ and SIRPα$_1$. HDX-MS, hydrogen deuterium exchange mass spectrometry; SIRP, signal-regulatory protein.

of HEFLB to monocytes from SIRPα$_1$/α$_1$ individuals (figure 3A,B) is probably due to SIRPβ1v1 and/or SIRPβ1v2 recognition by HEFLB (figure 1A,B) known to be expressed on these cells.[57] In addition, 1H9 was also found to be a poor inhibitor of CD47-bead binding to monocytes of SIRPα$_1$/α$_1$ origin (figure 3A,B). BYON4228 also inhibited the interaction between SIRPα and CD47 to background levels when using the promonocytic human cell line U937 expressing endogenous SIRPα (figure 3C).

To study the effect of BYON4228 binding on CD47-induced SIRPα-signaling, the DiscoverX PathHunter SIRPα Signaling Bioassay was used. This technology uses CD47-deficient Jurkat cells that express SIRPα$_{BIT}$ linked to an β-galactosidase enzyme donor. On ligation with cellular CD47 the enzyme acceptor-linked SHP-1 protein is recruited to SIRPα, and an active β-galactosidase enzyme is formed. Thus, the degree of SIRPα signaling can be measured in a quantitative fashion. We used Raji, SK-BR-3 and A431 cancer cells as a source of cellular CD47-ligand and found that all these cells induced a chemiluminescent signal on co-incubation with the PathHunter SIRPα-expressing Jurkat cells (figure 3D and online supplemental figure S1D). All antibodies tested were able to dose-dependently inhibit SIRPα$_{BIT}$ signaling induced by all three tested CD47-expressing cell lines to background levels (figure 3D and online supplemental figure S1D). Overall, these results show that BYON4228 binds to a conserved epitope that overlaps with the CD47-binding site on SIRPα, and constitutes a pan-allelic SIRPα blocking antibody that inhibits CD47 binding and CD47-induced SIRPα-signaling.

BYON4228 lacks binding to human T-cell expressed SIRPγ

The binding of BYON4228 and other antibodies to SIRPγ was then investigated. BYON4228 displayed no detectable binding to SIRPγ when transiently expressed on ExpiCHO-S cells and negligible/no binding to SIRPγ expressed as a soluble protein (figure 4A, table 3). In line with earlier reports,[54] HEFLB also lacked binding to SIRPγ, whereas SIRPAB-11 showed potent binding to SIRPγ-expressing cells (figure 4A). We furthermore noted, in contrast to an earlier report,[49] that 1H9 also displayed SIRPγ binding when expressed on ExpiCHO-S cells. In line with this, 1H9 also demonstrated binding to SIRPγ-expressing T cells, although with lower potency than SIRPAB-11 (figure 4B,C). Importantly, BYON4228 lacked binding to T cells altogether (figure 4B,C). CD47 is a known ligand for both SIRPα and SIRPγ[45] and indeed, CD47-coated beads showed binding to T cells of most donors. The antibodies 1H9 and SIRPAB-11 blocked CD47-bead binding to T cells, while BYON4228 and HEFLB did not alter this binding (figure 4B,C). Overall, these results show that BYON4228 lacks binding to T-cell expressed SIRPγ and accordingly does not affect CD47 binding to SIRPγ on T cells.

BYON4228 promotes ADCC and ADCP of therapeutic mAbs in a pan-allelic fashion

We then continued to investigate the functional activity of BYON4228 with respect to tumor cell killing. We first studied the impact of BYON4228 on neutrophil-mediated ADCC induced by anti-TAAs. GM-CSF-activated neutrophils were able to kill SK-BR-3 breast cancer tumor cells opsonized with trastuzumab. Addition of BYON4228 potentiated this killing in a dose-dependent and pan-allelic fashion (figure 5A–C), with an average 2.5-fold to 3.0-fold enhancement (figure 5C) of trastuzumab-induced killing at saturating BYON4228 concentrations. ADCC enhancement by BYON4228 appeared most potent (ie, lower EC$_{50}$ values) when neutrophils were of SIRPα$_1$/α$_1$ origin (EC$_{50}$ geomean of 0.10 µg/mL vs 0.19 and 0.26 for SIRPα$_{BIT}$/α$_1$ and SIRPα$_{BIT}$/α$_{BIT}$ donors, respectively). However, at saturating levels of BYON4228, ADCC enhancement was not significantly different between different SIRPα genotyped donors (figure 5C). As expected, the SIRPα$_{BIT}$-specific antibody HEFLB was unable to potentiate trastuzumab-ADCC by SIRPα$_1$/α$_1$ homozygous neutrophils. In addition, trastuzumab-ADCC enhancement of HEFLB by SIRPα$_{BIT}$/α$_1$ neutrophils was limited (1.3-fold by SIRPα$_{BIT}$/α$_1$ donors vs 3.0-fold by SIRPα$_{BIT}$/α$_{BIT}$ donors). 1H9 potentiated ADCC by SIRPα$_1$/α$_1$ neutrophils with limited efficacy (1.5-fold enhancement by SIRPα$_1$/α$_1$ donors vs 3.3-fold enhancement by SIRPα$_{BIT}$/α$_{BIT}$ donors), which was in line with its limited ability to antagonize CD47 binding to monocytes homozygous for SIRPα$_1$ (figure 3A,B). To further evaluate the broadness of its therapeutic applicability, we also determined whether BYON4228 could enhance the ADCC activity of neutrophils towards other target cells, including cetuximab-opsonized and

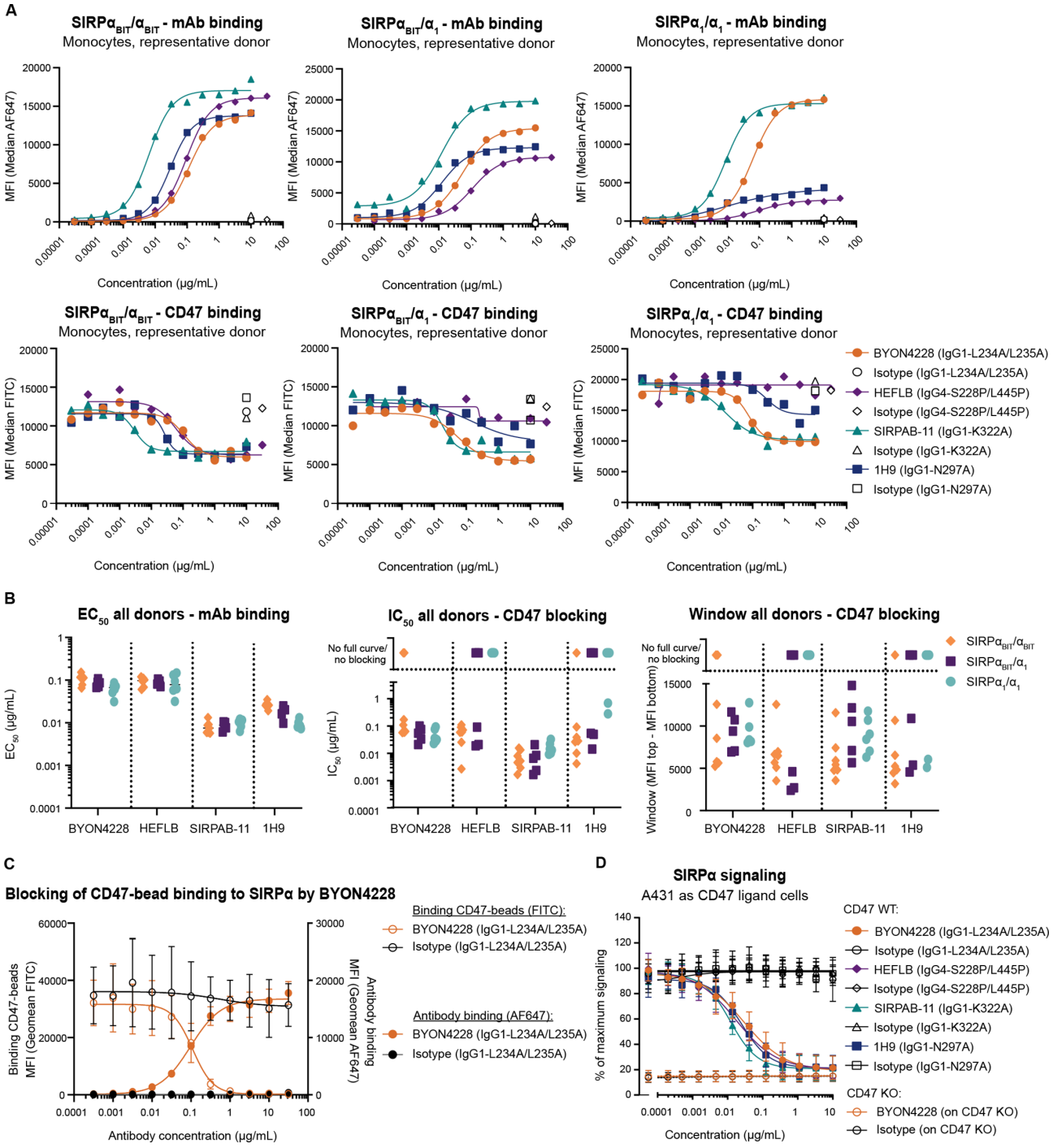

Figure 3 BYON4228 competitively blocks binding of CD47 to SIRPα. (A,B) anti-SIRP mAb binding and blockade of CD47 binding to primary monocytes. Indicated fluorescently labeled antibodies were incubated with primary peripheral blood mononuclear cells for 30 min, and then, fluorescently labeled CD47-coated beads were added. mAb binding and CD47 binding was measured on gated CD14-positive monocytes. (A) Top row depicts mAb binding and bottom row depicts CD47 binding to monocytes of representative donors with indicated SIRPα genotypes. (B) Overview of the mAb binding EC_{50} values (geomeans are depicted), blocking of CD47 binding IC_{50} values, and CD47 blocking windows (Δ MFIs) per antibody of all donors tested (seven SIRPα$_{BIT}$/$_{BIT}$, five SIRPα$_{BIT}$/α$_1$, and six SIRPα$_1$/α$_1$ donors). No IC_{50} values could be calculated from donors with incomplete curve saturation or no response as indicated in the graph. Donors that did not show a window for CD47 blocking were also indicated in the graph. (C) Graph depicts binding of CD47 coated fluorescent beads to U937 cells (left y-axis, open symbols), incubated in the presence of a dose-range of BYON4228-AF647 or AF647-labeled isotype control (right y-axis, closed symbols). Results display average binding MFIs ±SD measured in the FITC or AF647 channel of N=3 independent experiments. (D) SIRPα signaling measured using the PathHunter Jurkat SIRPα signaling reporter cell line (DiscoverX), after co-incubation with CD47-expressing or knock-out (KO) A431 cells, in presence of a concentration-range of indicated antibodies. Results are shown as mean ±SD of N=6 independent experiments. FITC, fluorescein isothiocyanate; mAb, monoclonal antibody; MFI, median fluorescent intensities; SIRP, signal-regulatory protein.

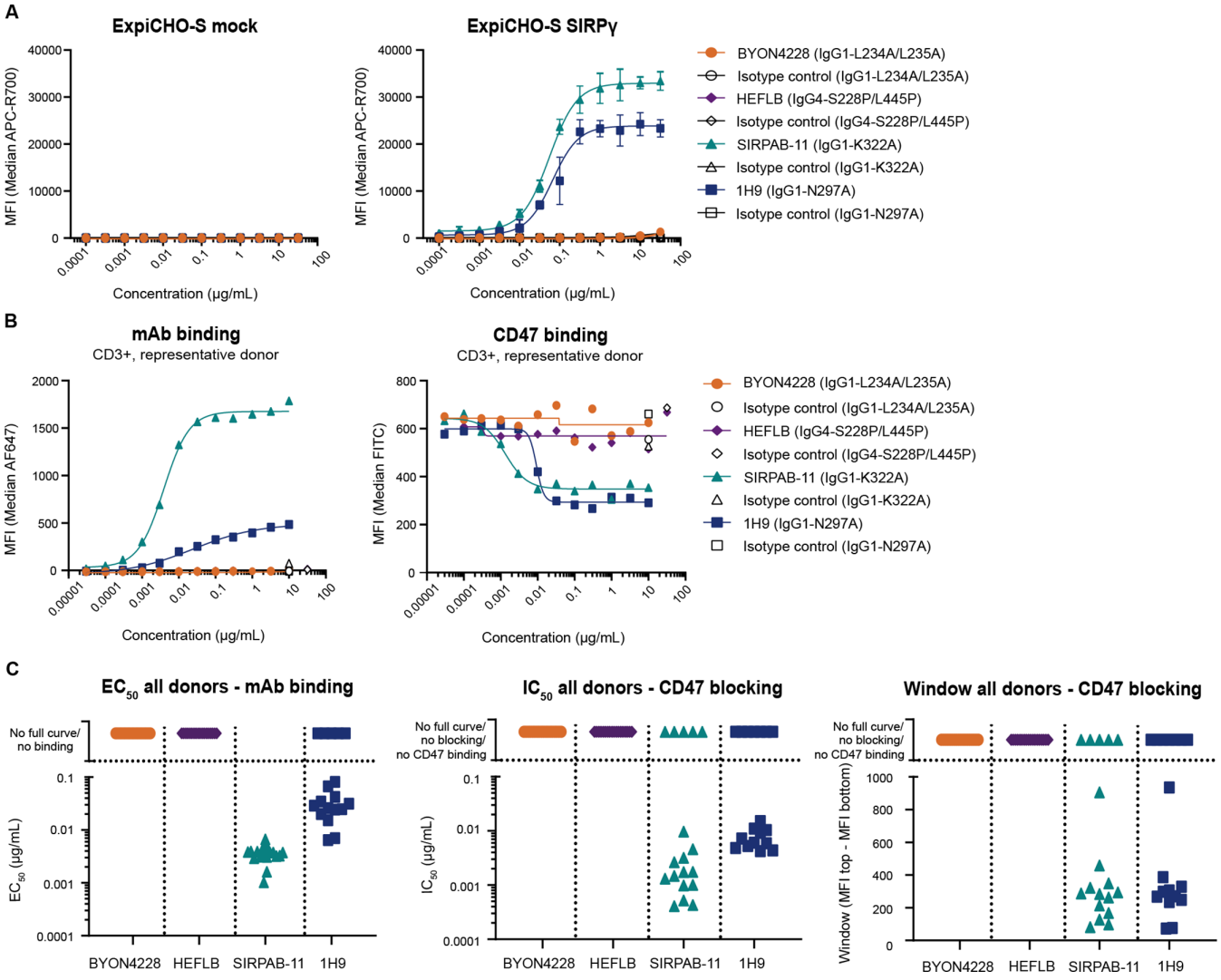

Figure 4 BYON4228 lacks binding to T-cell expressed SIRPγ. (A) Binding of indicated SIRPα antibodies and respective isotype control antibodies to ExpiCHO-S cells that transiently expressed SIRPγ or were mock transfected. Average MFI ±SD of N=3 independent experiments are depicted. (B, C) Anti-SIRP mAb binding and blockade of CD47 binding to primary CD3-positive cells. Indicated fluorescently labeled antibodies were incubated with primary peripheral blood mononuclear cells for 30 min, and then, fluorescently labeled CD47-beads were added. mAb binding and CD47 binding were measured on gated CD3-positive T cells. (B) The left graph depicts mAb binding and the right graph depicts CD47 binding of representative donors. (C) Overview of mAb binding EC_{50} values, CD47 binding IC_{50} values and CD47 blocking windows (Δ MFI) for all donors tested (N=18 donors). No EC_{50} and IC_{50} values could be calculated from donors with incomplete curve saturation or no response as indicated in the graph. While all T-cell donors showed SIRPAB-11 and 1H9 binding and thus most likely expressed SIRPγ, for four of these donors, no T-cell binding of CD47-labeled beads could be demonstrated. Therefore, no IC_{50} value and window could be determined for these four donors and as such they are shown in the top part of the graph (no CD47 binding) together with donors that showed no CD47-blocking or incomplete curve saturation. APC, allophycocyanin; ExpiCHO-S, Expi Chinese hamster ovary-S; mAb, monoclonal antibody; MFI, median fluorescent intensities; SIRP, signal-regulatory protein.

panitumumab-opsonized cancer cell lines (online supplemental figure S2). Both panitumumab (IgG2) and cetuximab (IgG1) alone were able to induce neutrophil ADCC towards the EGFR-expressing epidermoid tumor cell line A431 in a dose-dependent fashion (online supplemental figure S2A–C). BYON4228 enhanced the killing of both anti-EGFR antibodies (online supplemental figure S2E). We also tested panitumumab-induced and cetuximab-induced neutrophil ADCC of the colorectal cancer (CRC) cell line SW48 (online supplemental figure S3). Here, panitumumab consistently led to higher levels of neutrophil-induced killing when compared with cetuximab (4.5-fold vs 1.8-fold, respectively) (online supplemental figure S3C). Again, BYON4228 was able to enhance both panitumumab-induced and cetuximab-induced killing of the CRC cell line SW48 (1.7-fold vs 1.6-fold, respectively) (online supplemental figure S3E). We further tested isogenic SW48 cell lines containing frequently occurring constitutively activating mutations downstream the EGFR signaling pathway (Kirsten rat sarcoma virus (KRAS) G12D, KRAS G13D, rapidly accelerated fibrosarcoma B-type (BRAF) V600E). As expected,

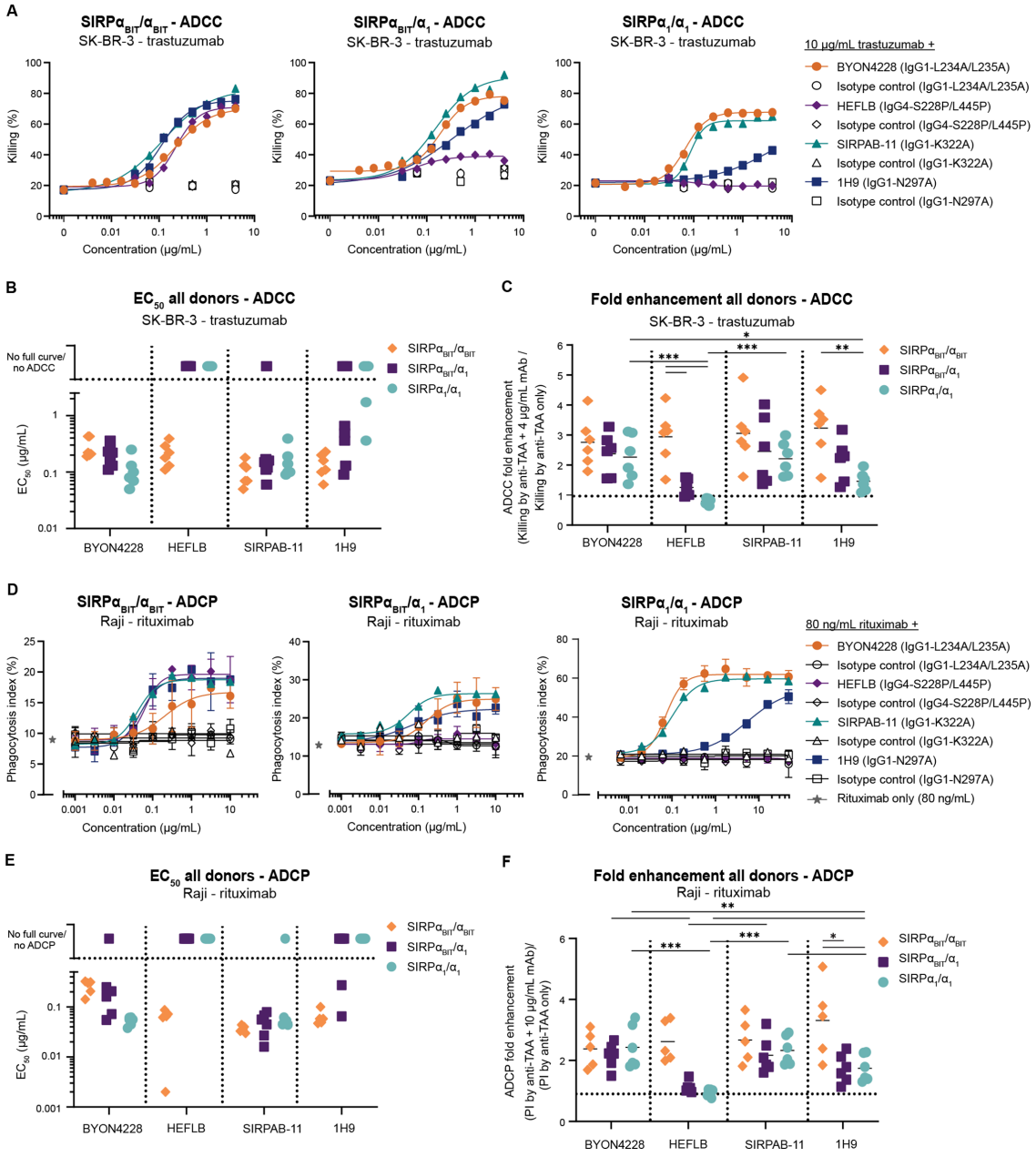

Figure 5 BYON4228 enhanced ADCC and ADCP of therapeutic mAbs in a pan-allelic fashion. (A–C) Neutrophil-mediated ADCC measured using the Cr-51 release assay after 4 hours incubation of target cells (SK-BR-3) and effector cells (primary granulocyte-macrophage colony-stimulating factor activated neutrophils) in the presence of a fixed dose of trastuzumab (10 µg/mL) and a concentration range of indicated antibodies or respective isotype controls. Donors tested: Six SIRPα$_{BIT}$/$_{BIT}$, eight SIRPα$_{BIT}$/α$_{1}$, and six SIRPα$_{1}$/α$_{1}$ donors. (A) Results show concentration-dependent SIRP-mAb induced % killing of SK-BR-3 cells by activated neutrophils of representative donors with indicated SIRPα genotypes. (B) SIRP-mAb induced ADCC EC$_{50}$ values of all donors. No EC$_{50}$ values could be calculated from donors with incomplete curve saturation, no response or incorrect curve-fitting as indicated in the graph. (C) SIRP-mAb induced ADCC fold enhancement of all donors. The means are depicted. The fold enhancement=(% killing at 10 µg/mL trastuzumab + 4 µg/mL anti-SIRPα mAb)/(% killing at 10 µg/mL trastuzumab). (D–F) Macrophage-mediated ADCP measured using confocal microscopy after 3 hours incubation of target cells (Raji) and effector cells (macrophages) in the presence of a fixed dose of rituximab (80 ng/mL) and a concentration range of indicated antibodies or respective isotype controls. Donors tested: Five SIRPα$_{BIT}$/$_{BIT}$, six SIRPα$_{BIT}$/α$_{1}$, and six SIRPα$_{1}$/α$_{1}$ donors. (D) Results show SIRP-mAb induced Phagocytosis Index (PI) of macrophages from representative donors with indicated SIRPα genotypes. (E) SIRP-mAb induced ADCP EC$_{50}$ values of all donors. No EC$_{50}$ values could be calculated from donors with incomplete curve saturation, no response or incorrect curve-fitting as indicated in the graph. (F) SIRP-mAb induced ADCP fold enhancement of all donors. The means are depicted. The fold enhancement=(PI at 80 ng/mL rituximab + 10 µg/mL anti-SIRP mAb)/(PI at 80 ng/mL rituximab). For C and F, * p<0.05, ** p<0.01, ***p<0.001; p>0.05 is not indicated. P values were calculated by one-way analysis of variance (ANOVA) for each genotype (comparing the different mAbs) and for each mAb (comparing the different genotypes) followed by Tukey's multiple comparisons test. ADCC, antibody-dependent cellular cytotoxicity; ADCP, antibody-dependent cellular phagocytosis; mAb, monoclonal antibody; SIRP, signal-regulatory protein; TAA, tumor-associated antigen.

the EGFR pathway mutant cell lines were killed by neutrophils after opsonization with panitumumab and this was further enhanced by BYON4228 (online supplemental figure S3F–H), although overall levels of killing were variable between the different cell lines, probably as a result of differences in EGFR expression levels (online supplemental table S1). The observation that BYON4228 was able to enhance the efficacy (ie, maximum killing) of panitumumab in all tested cell lines (online supplemental figure S3F–H), implies that therapeutic efficacy of a combination of panitumumab and BYON4228 might even be expected in patients that bear the indicated and other known growth-promoting mutations downstream the EGFR signaling pathway, an indication for which cetuximab and panitumumab are currently not registered/recommended.

The capacity of BYON4228 to enhance macrophage-mediated-ADCP induced by anti-TAAs was studied. CD20-expressing CellTrace Far Red labeled Raji cells (Burkitt's lymphoma) were opsonized with rituximab and phagocytosis by monocyte-derived macrophages was assessed using confocal microscopy. To ensure phagocytosis, anti-CD19 was used as a counterstain and only CD19-negative Raji cells entirely engulfed by macrophages (ie, truly phagocytosed) were counted. Rituximab-induced phagocytosis was increased by BYON4228 in a dose-dependent fashion (figure 5D–F). This synergistic effect was detected with all macrophages, irrespective of their SIRPα genotype. We noted that BYON4228 showed higher potency (ie, lower EC_{50}) when macrophages were of $SIRP\alpha_1/\alpha_1$ origin compared with $SIRP\alpha_{BIT}/\alpha_{BIT}$ macrophages (EC_{50} of 0.05 vs 0.25 µg/mL, respectively) (figure 5E). However, the fold enhancement of the Phagocytosis Index of rituximab-induced phagocytosis by $SIRP\alpha_{BIT}/\alpha_{BIT}$ donors at saturating 10 µg/mL was not significantly different when compared with $SIRP\alpha_{BIT}/\alpha_1$ or $SIRP\alpha_1/\alpha_1$ donors (figure 5F). The $SIRP\alpha_{BIT}$-specific blocking antibody HEFLB was again not or only hardly capable of enhancing rituximab-induced phagocytosis by $SIRP\alpha_1$-homozygous or heterozygous macrophages, respectively. Similarly, 1H9 showed limited efficacy and potency for phagocytosis enhancement by $SIRP\alpha_1/\alpha_1$ and $SIRP\alpha_{BIT}/\alpha_1$ macrophages. Remarkably similar results were found when Daudi cells (non-Hodgkin's lymphoma) were used in combination with daratumumab (anti-CD38) (online supplemental figure S4A–C). We also studied phagocytosis in an alternative live-cell imaging-based phagocytosis assay that relied on pHrodo-labeled tumor cells turning bright red on phagocytosis (movie in online supplemental files 7 and 8). The advantage of this method was that no counterstain (anti-CD19) was required to determine phagocytic uptake of the target cell. We again tested daratumumab-induced phagocytosis of Daudi cells and found that BYON4228 strongly enhanced uptake of target cells (online supplemental figure S4D–F). The overall potency of BYON4228 (ie, geomean EC_{50} for all donors, irrespective of the SIRPα genotype) was 0.9 µg/mL in the live-cell imaging pHrodo ADCP assay (N=16) compared with 0.09 µg/mL in the confocal ADCP assay (N=12) (online supplemental figure S4), suggesting the live-cell imaging assay was less sensitive, but was a reproducible orthogonal assay nevertheless. Using the live-cell imaging assay we furthermore studied ADCP of the CRC cell line HT-29 and found that BYON4228 was able to enhance panitumumab-induced and cetuximab-induced phagocytosis (online supplemental figure S5). Altogether, BYON4228 showed functional activity in both neutrophil ADCC and macrophage ADCP assays, indicating its ability to enhance tumor cell killing by myeloid cells.

The BYON4228 silenced Fc tail avoids opsonization and destruction of SIRPα-expressing myeloid cells

With respect to the therapeutic activity of anti-SIRPα antibodies, which relies on anticancer activity of SIRPα-expressing myeloid immune effector cells, it would be undesirable if such SIRPα-expressing cells were depleted through anti-SIRPα Fc mediated processes like CDC, ADCC or ADCP in vivo. Such depletion might compromise both the safety and efficacy of the therapeutic anti-SIRPα antibody. To prevent this, BYON4228 was designed with an IgG1 Fc tail containing L234A/L235A mutations in the Fc tail (abbreviated as 'LALA'-tail). As expected, BYON4228 displayed strongly decreased binding to FcγRs when compared with its counterpart with wild type (WT) IgG1 backbone without the LALA mutations (IgG1) (online supplemental table S2). Consistent with this, BYON4228 was unable to induce macrophage-mediated phagocytosis of the SIRPα-expressing acute myeloid leukemia (AML) tumor cell line OCI-AML2, whereas the WT IgG1 variant (BYON5664) and anti-CD47 WT IgG1 clearly induced phagocytosis (figure 6A–C). Notably, SIRPAB-11, which contains an IgG1-tail with the K322A modification (designed for reduction of complement activation[58]), also induced ADCP of the OCI-AML2 cells. In line with its inability to induce phagocytosis of SIRPα-positive cells, BYON4228 did not induce NK cell-mediated ADCC of SIRPα-expressing target cells, whereas NK cell induced ADCC was observed by the IgG1 variant (online supplemental figure S6A). Both BYON4228 and its IgG1 variant did not induce CDC of the SIRPα-expressing cell lines U937 and MOLM-13, whereas anti-CD47 (IgG1) induced potent lysis of these cells after incubation with active serum (online supplemental figure S6B). Overall, these data show that the silent Fc tail of BYON4228 prevents destruction of SIRPα-expressing cells by different immune-mediated mechanisms.

Optimal enhancement of anti-TAA-induced ADCC and ADCP by BYON4228 is independent of its Fc functionality

For optimal efficacy, it was suggested previously that the Fc tail of SIRPα-blocking antibodies should not be able to bind to FcγRs on myeloid effector cells in cis to avoid competition with the tumor-opsonizing antibody-FcγR interaction and hence reduced tumor cell destruction, a phenomenon also known as the 'scorpion effect'.[51 59] To examine the influence of the Fc tail for BYON4228

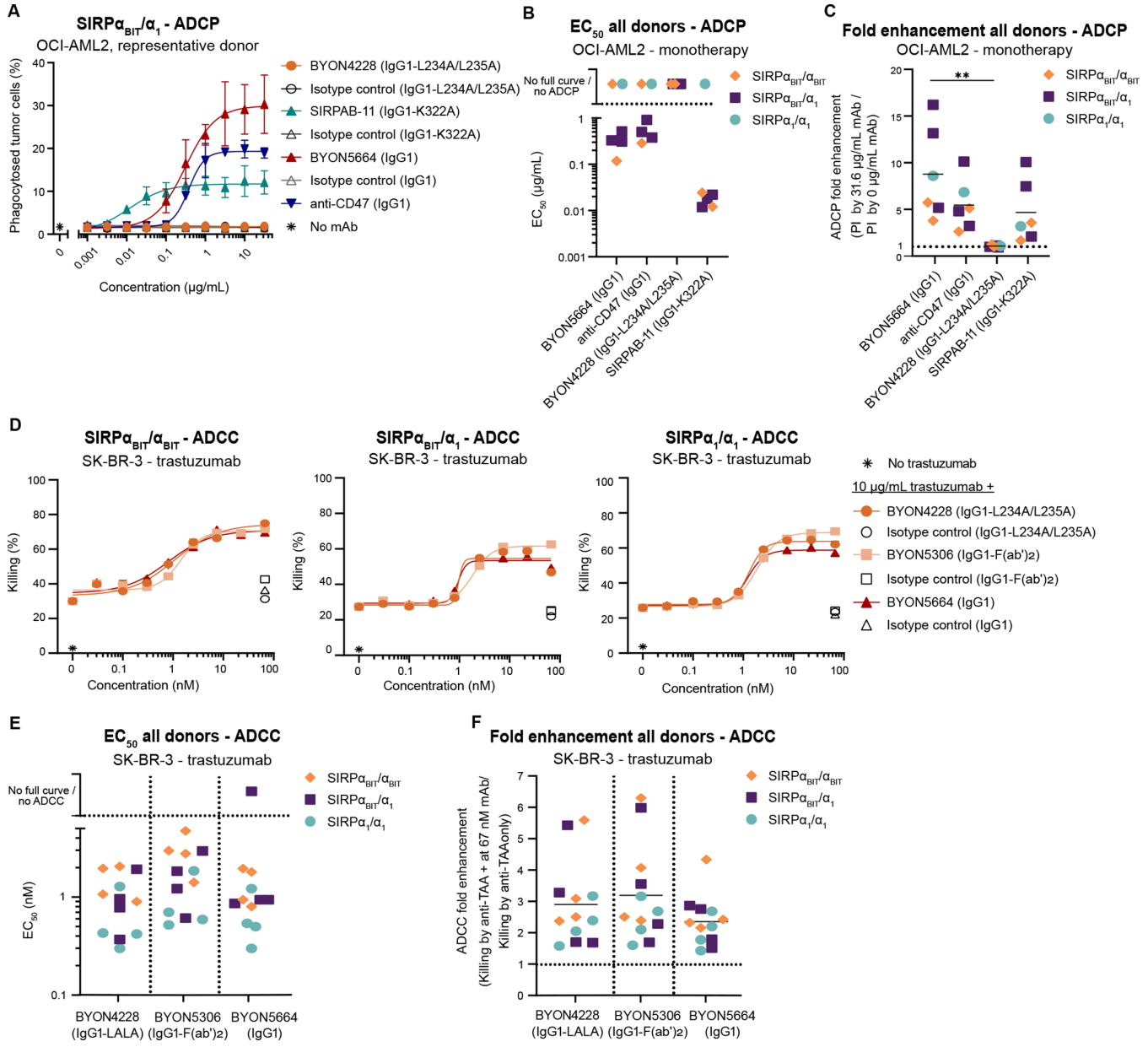

Figure 6 Potent and efficacious enhancement of anti-TAA-induced ADCC and ADCP with BYON4228 having a hIgG1-L234A/L235A Fc tail. (A–C) Macrophage mediated ADCP measured using the live-cell imaging pHrodo ADCP assay after incubation of target cells (OCI-AML2) and effector cells (macrophages) in the presence of a concentration range of indicated antibodies or respective isotype controls. BYON5664 contains the variable domains of BYON4228 but has a wildtype IgG1 constant domain with wildtype effector functions. Donors tested: Two SIRPα$_{BIT}$/α$_{BIT}$, three SIRPα$_{BIT}$/α$_1$, and one SIRPα$_1$/α$_1$ donors. (A) Results show % phagocytosed tumor cells by macrophages from a representative donor. No mAb=effector+target cells only. (B) ADCP EC$_{50}$ values of all donors. No EC$_{50}$ values could be calculated from donors with incomplete curve saturation, no response or incorrect curve-fitting as indicated in the graph. (C) The ADCP fold enhancement of all donors. The means are depicted. The fold enhancement=(% phagocytosed cells at 31.6 µg/mL anti-SIRP)/(% phagocytosed cells at effector+target). (D–F) Neutrophil-mediated ADCC measured using the Cr-51 release assay after 4 hours incubation of target cells (SK-BR-3) and effector cells (primary granulocyte-macrophage colony-stimulating factor activated neutrophils) in the presence of a fixed dose of trastuzumab (10 µg/mL) and a concentration range of indicated antibodies or respective isotype controls. BYON5306 is the F(ab')$_2$ fragment of BYON4228. Donors tested: four SIRPα$_{BIT}$/α$_{BIT}$, four SIRPα$_{BIT}$/α$_1$, and four SIRPα$_1$/α$_1$ donors. (D) Results show % killing of SK-BR-3 cells by activated neutrophils of representative donors with indicated SIRPα genotypes. (E) SIRP-mAb or -F(ab')$_2$ induced ADCC EC$_{50}$ values of all donors. No EC$_{50}$ values could be calculated from donors with incomplete curve saturation, no response or incorrect curve-fitting as indicated in the graph. (F) SIRP-mAb induced ADCC fold enhancement of all donors. The means are depicted. The fold enhancement=(% killing at 10 µg/mL trastuzumab+67 nM anti-SIRPα mAb)/(% killing at 10 µg/mL trastuzumab). For C and F, *p<0.05, **p<0.01, ***p<0.001; p>0.05 is not indicated. P values were calculated by one-way analysis of variance (ANOVA) followed by Tukey's multiple comparisons test. ADCC, antibody-dependent cellular cytotoxicity; ADCP, antibody-dependent cellular phagocytosis; AML, acute myeloid leukemia; mAb, monoclonal antibody; SIRP, signal-regulatory protein; TAA, tumor-associated antigen.

for optimal in vitro ADCC and ADCP, we generated a fragment antigen-binding region ($F(ab')_2$) version of BYON4228, which was still able to block CD47-SIRPα axis signaling to the same extent as intact BYON4228 (online supplemental figure S6C). We performed similar side-by-side comparisons to determine enhancement of anti-TAA-induced neutrophil ADCC. BYON4228 was able to enhance trastuzumab-induced ADCC of SK-BR-3 cells with a similar potency and efficacy when the Fc tail was lacking (figure 6D–F). Even when the Fc tail of BYON4228 was replaced with a human WT IgG1 tail (IgG1), ADCC potency and efficacy of enhancement were similar (figure 6D–F). Similar results were also obtained when the BYON4228 variants were tested for enhancement of cetuximab-induced ADCC of A431 cells (online supplemental figure S6D–F). The $F(ab')_2$ fragment of BYON4228 was compared with BYON4228 in the rituximab-induced macrophage ADCP assay. Here again, the ability to enhance rituximab-induced phagocytosis of Raji cells was essentially indistinguishable from that of BYON4228 (online supplemental figure S7A–C). Finally, daratumumab-induced ADCP enhancement of Daudi cells was identical for BYON4228 or its $F(ab')_2$ (online supplemental figure S7D–F). Overall, these data show that neither BYON4228 nor its WT IgG1 variant suffer from the 'scorpion effect', and therefore BYON4228 provides optimal enhancement of antibody-dependent tumor cell destruction by both neutrophils and macrophages.

BYON4228 improves the efficacy of rituximab in human SIRPα$_{BIT}$-scid mice in vivo

Like most anti-human SIRPα blocking antibodies, BYON4228 does not cross-react with mouse SIRPα (data not shown). To study efficacy of BYON4228 in vivo, we generated mice that expressed human SIRPα$_{BIT}$ from the Rosa26 promotor only in myeloid cells due to Cre-mediated excision of a STOP cassette (Rosa26-stop^{flox}human SIRPα$_{BIT}$ × *Cebpa*$^{Cre/+}$,[60] named huSIRPα$_{BIT}$ mice). Western blot analysis confirmed the presence of the human SIRPα glycoprotein in *Cebpa*$^{Cre/+}$ mice in conjunction with the endogenous mouse SIRPα (online supplemental figure S8A). Flow cytometry analysis showed that the mice indeed expressed human SIRPα$_{BIT}$ on monocytes and neutrophils (online supplemental figure S8B,C). Furthermore, murine neutrophils that expressed human SIRPα$_{BIT}$ enhanced trastuzumab-induced ADCC of SK-BR-3 cells in presence of an anti-SIRPα antibody (online supplemental figure S8D,E), demonstrating proper functionality of the huSIRPα$_{BIT}$ transgene in mice.

First, BYON4228 pharmacokinetic (PK) studies were performed in C57Bl/6 mice and in huSIRPα$_{BIT}$ mice. In C57Bl/6 mice, a low clearance of BYON4228 was noted, while in huSIRPα$_{BIT}$ mice, a threefold higher clearance (based on area under the curve $(AUC)_{last}$) was observed after intravenous or IP administration of a low dose (3 mg/kg) BYON4228 (online supplemental figure S8F,G and online supplemental table S3 and S4). This difference in drug clearance is most likely due to target-mediated drug disposition (TMDD). In huSIRPα$_{BIT}$ mice, the drug elimination via TMDD could be saturated by high doses (intravenous) or repeat dosing (IP) of BYON4228, leading to prolonged high plasma BYON4228 levels (online supplemental figure S8F–H).

Next, antitumor efficacy of rituximab alone or in combination with BYON4228 was studied in huSIRPα$_{BIT}$-scid mice SC xenografted with Raji tumors. No significant effects of BYON4228 alone on tumor growth were observed (one experiment, N=9 mice/group, data not shown). Rituximab treatment at 1 mg/kg significantly inhibited growth of Raji cells in huSIRPα$_{BIT}$-scid mice and this effect could be enhanced by combination treatment with BYON4228 at 5 mg/kg (figure 7A), one of two independent studies shown, N=11 mice/group). These results show that the huSIRPα$_{BIT}$-scid mouse model can be employed to study efficacy of anti-SIRPα antibodies in

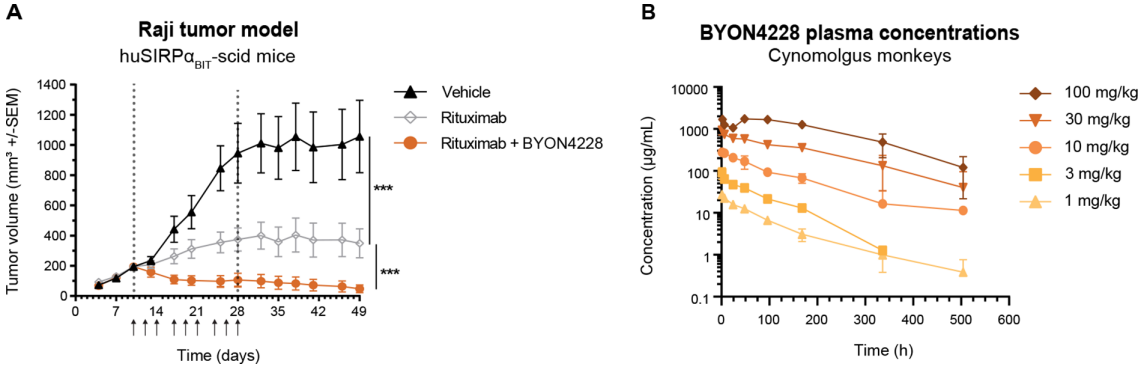

Figure 7 BYON4228 potentiates the antitumor activity of rituximab in vivo and pharmacokinetic evaluation of BYON4228 in cynomolgus monkeys. (A) Growth curve of Raji cells (subcutaneous) in female huSIRPα$_{BIT}$-scid mice treated IP with vehicle, rituximab monotherapy, or rituximab in combination with BYON4228. All compounds were administered IP three times a week (indicated by arrows between dotted lines). Rituximab was used at 1 mg/kg for monotherapy and in combination with 5 mg/kg BYON4228. N=11 per group. Statistical analysis of area under the curve from randomization to end of study; *** p<0.001, Dunnett's multiple comparison test. (B) Mean BYON4228 plasma concentrations in cynomolgus monkey after a single intravenous infusion of BYON4228 (N=2 (one female and one male) ±SD/dose group). IP, intraperitoneal; SIRP, signal-regulatory protein; scid, severe combined immunodeficiency.

vivo and, most importantly, that BYON4228 can improve tumor clearance when combined with rituximab. These data are in line with Murata *et al*, who demonstrated enhancement of the inhibitory effect of rituximab by anti-human SIRPα antibody on the growth of tumors formed by Raji cells in other human SIRPα transgenic mice.[61]

BYON4228 has a favorable preclinical safety profile

We assessed the safety of BYON4228 in vitro. BYON4228 did not display hemolytic activity, it did not induce red blood cell (RBC) clumping and it was compatible with human plasma in vitro (data not shown). At concentrations of 1 up to 100 µg/mL, BYON4228 did not induce any biologically significant increases in a panel of 18 cytokines/chemokines measured (data not shown). A toxicological evaluation of BYON4228 was performed in cynomolgus monkeys. We noticed that BYON4228 displayed potent binding to SIRPα-positive granulocytes of most cynomolgus monkeys (online supplemental figure S9A,B). Individual monkeys that displayed no or very poor BYON4228 binding were deselected for toxicity studies. The selected individuals had an average 3.5-fold more potent binding (3.5-fold lower EC_{50}) compared with that in man (0.03 µg/mL, online supplemental figure S9B vs 0.09 µg/mL, figure 1D), supporting the relevance of cynomolgus monkey for the human risk assessment of BYON4228. Intravenous infusion of BYON4228 was well tolerated as a single dose up to 100 mg/kg. PK profiles in monkeys showed almost dose linear increase in exposure. One week after dosing, variability is observed in the PK curves due to the induction of immunogenicity as was confirmed by the observation of anti-drug antibodies (figure 7B, online supplemental table S5 and data not shown). In the 5-cycle repeated dose toxicity study in monkey, where 3, 10 or 30 mg/kg BYON4228 was infused intravenously one time a week, BYON4228 showed comparable PK profiles and was well tolerated with no adverse effects on body weight and no clinical evidence of toxicity including safety pharmacology endpoints (cardiovascular, respiratory, and central nervous system) (data not shown). In addition, no effects on hemoglobin levels, RBC count or platelets were noted (online supplemental figure S9C–E). When comparing the measured SIRPα receptor occupancy (RO) data with the observed exposure levels, the data show that >80%–90% RO (needed for 100% efficacy in ADCC and ADCP assays in vitro, data not shown) can be reached at plasma concentrations around 2 µg/mL BYON4228 based on limited data. The mean C_{trough} of BYON4228 following the first dose in the 5-cycle toxicity study ranged from 15.8 µg/mL to 285 µg/mL for the 3–30 mg/kg doses indicating that the >80% RO had been reached over the entire dosing interval. Based on the 5-cycle study, the No Adverse Effect Level (NOAEL) was considered to be the highest dose tested, 30 mg/kg. At this repeated dose, the exposure is 165,000 hours × µg/mL for males and 179,000 hours × µg/mL for females.

DISCUSSION/CONCLUSION

The CD47-SIRPα myeloid immune checkpoint has been identified as a promising therapeutic target to promote tumor destruction in combination with anti-TAAs and other therapeutics.[9 38] Blockade of CD47-SIRPα signaling can stimulate destruction of antibody-opsonized cancer cells by innate immune cells, in particular by macrophage ADCP and neutrophil ADCC. Furthermore, disruption of CD47-SIRPα interactions triggers adaptive T cell-mediated anticancer immunity, probably, at least in part, by enhancing cross-presentation by SIRPα-expressing dendritic cells. Currently, a number of agents targeting CD47 or SIRPα are in clinical development. The vast majority of these agents are targeting CD47 and the most advanced ones have already shown encouraging safety/efficacy profiles in early clinical studies.[36 37 39 41] Nevertheless, as outlined above there are a number of disadvantages of targeting CD47, and this may therefore not be the most optimal and selective way to antagonize CD47-SIRPα interactions therapeutically. Notably, the disruption of CD47-SIRPγ interactions, which are critical for T-cell extravasation and activation,[34 46–48] might curtail durable adaptive antitumor immunity.

As an alternative strategy, therapeutic agents have been developed that target SIRPα[29 34 49–53 55] and at present four of such drugs are, or have been, in early clinical development. Preclinical data of HEFLB, SIRPAB-11, and 1H9, most likely corresponding to BI 765063 (formerly OSE-172), BMS-986351 (anzurstobart, formerly CC-95251), and GS-0189 (formerly FSI-189) (table 1), respectively, have been reported.[34 49 58] However, we have shown here that these SIRPα blocking antibodies, like several others that have been reported,[50–53 55] either fail to recognize both of the two SIRPα polymorphic variants present in the human population, or they cross-react with SIRPγ.

Here we preclinically characterize BYON4228, a novel anti-SIRPα antibody, and perform direct in vitro comparisons with HEFLB, SIRPAB-11, and 1H9. Our results identify BYON4228 as a highly differentiating antibody, which recognizes both of the two polymorphic variants $SIRP\alpha_{BIT}$ and $SIRP\alpha_1$. BYON4228 efficiently inhibits CD47 binding to primary myeloid cells from individuals with all three genotypes (ie, $SIRP\alpha_{BIT}$-homozygotes and $SIRP\alpha_1$-homozygotes and $SIRP\alpha_{BIT}$/$SIRP\alpha_1$-heterozygotes). The antagonistic activity of BYON4228 can be explained by direct competition with CD47 binding, as the BYON4228 epitope strongly overlaps with the previously described CD47 binding site on both of the SIRPα variants.[21] In line with this, BYON4228 prevents inhibitory signaling via the CD47-SIRPα axis, and promotes neutrophil ADCC and macrophage ADCP using immune effector cells from individuals of all three SIRPα genotypes. In contrast, HEFLB lacks binding to $SIRP\alpha_1$ and, as a consequence, the ability to reduce CD47 binding to $SIRP\alpha_1$ homozygous myeloid cells, and clearly fails to enhance ADCC and ADCP by $SIRP\alpha_1$ homozygous myeloid immune effector cells. Notably, HEFLB also appears to be only a partial inhibitor of CD47 binding by $SIRP\alpha_{BIT}$/$SIRP\alpha_1$

heterozygote myeloid cells, and, if anything, only a weak stimulator of ADCC and ADCP, mediated by, respectively, neutrophils and macrophages from such heterozygous individuals. These findings are also supported by previous reports.[51 55] These properties will likewise compromise the applicability of BI 765063/OSE-172, the probable corresponding agent of HEFLB in clinical development, in more than half (range: 51–88%) of all major ethnic patient populations.[50] Surprisingly, and in contrast to its reported pan-allelic functionality,[49] our data revealed that 1H9, and likewise its putative clinical equivalent GS-0189/FSI-189, exhibits only weak binding to SIRPα$_1$ on primary myeloid cells and it displays only partial inhibition of CD47 binding to SIRPα$_1$/α$_1$ homozygote cells accordingly. In contrast to this, Liu *et al* reported comparable binding of 1H9 to plate-coated soluble SIRPα$_1$-Fc and SIRPα$_{BIT}$ -Fc proteins. Indeed, we also noted similar binding potency of 1H9 to SIRPα$_1$ and SIRPα$_{BIT}$ expressed on ExpiCHO-S cells at high levels. However, the poor binding of 1H9 to SIRPα$_1$ become apparent when using primary human monocytes. Consistent with this, we noted limited potency of 1H9 when using SIRPα$_1$-homozygous cells in ADCC/ADCP assays using various target cell lines and anti-TAA combinations with many different donors, while Liu *et al* showed enhancement of cetuximab-induced ADCP of HT-29 cells by macrophages derived from SIRPα$_1$/α$_1$ donors, although only two donors were reported. The first-in-human study with GS-0189/FSI-189 (NCT04502706) was terminated after inclusion of a limited number of patients.

We also studied binding of the different mAbs to SIRPγ, a closely related homolog of SIRPα. BYON4228 lacked binding to SIRPγ, nor did affect CD47 binding to SIRPγ-expressing T cells. This may, as indicated, be instrumental to preserve optimal antitumor T-cell immunity. Instead, SIRPAB-11 and 1H9, and likewise their respective putative clinical equivalents BMS-986351/CC-95251 and GS-0189/FSI-189, clearly recognize SIRPγ, and also inhibit CD47 binding to primary T cells. While 1H9 was described not to bind to T cells,[49] only a narrow window of detection for the positive control was evident in the reported ELISA, possibly explaining the discrepancy with our findings.

BYON4228 was engineered with a modified L234A/L235A IgG1 Fc tail with strongly reduced Fc receptor binding to avoid non-desirable immune-mediated elimination of SIRPα-expressing myeloid cells,[62] which could both undermine the antitumor promoting effects of the drug, as well as cause toxicity, for instance by increasing susceptibility to infections. Indeed, the L234A/L235A modification prevented macrophage ADCP and NK ADCC towards SIRPα-positive cells in the presence of BYON4228 as a single agent. In contrast, SIRPAB-11, which has been modified to reduce complement activation, but exhibits normal Fc receptor binding[63] (and data not shown), demonstrates macrophage ADCP of SIRPα-positive cells. This may also be relevant in vivo in human patients, as the first results reported with the corresponding BMS-986351/anzurstobart/CC-95251 have demonstrated treatment-related ≥grade 3 neutropenia in 9 of 17 (53%) resistant/refractory patients with non-Hodgkin's lymphoma treated with escalating doses of the antibody.[64] It seems reasonable to assume that this is related to the high Fc receptor binding capacity of this particular anti-SIRPα antibody.

For some anti-SIRPα antibodies it has been reported that having a functional Fc region also compromises their ability to promote anti-TAA-dependent elimination of tumor cells.[51 55] In particular, it was postulated that the Fc tail of these SIRPα-bound antibodies have interactions with Fc receptors on myeloid effector cells in cis and therefore compete with anti-TAA Fc receptor binding, a phenomenon also known as the 'Scorpion-effect'.[51 59 65] Interestingly, the IgG1-L234A/L235A modification of BYON4228 was not necessary for optimal functionality, since a version equipped with a WT IgG1 Fc was equally potent and efficacious to enhance neutrophil ADCC. Moreover, complete elimination of the Fc effector functions using BYON4228 F(ab')$_2$ did not improve the performance of BYON4228 either. Thus, the Fc tail of BYON4228 has an optimal design for enhancing anti-TAA-dependent cancer cell destruction, while ensuring preservation of the normal myeloid immune effector cell populations.

Apart from the above in vitro properties our results also demonstrate efficacy of BYON4228 in an in vivo Raji B-cell lymphoma xenograft model in scid mice engineered to express human SIRPα$_{BIT}$ on myeloid cells. In particular, BYON4228 enhanced the antitumor activity of the anti-CD20 mAb rituximab. These results are in line with other studies with anti-SIRPα antibodies.[61] BYON4228 also displayed a favorable toxicity profile. Treatment of cynomolgus monkeys with BYON4228 up to 100 mg/kg (single dose) and up to 30 mg/kg (repeated dosing), which demonstrated complete RO on SIRPα-positive blood cells did not show any adverse effects, including the absence of anemia and thrombocytopenia. The latter contrasts with results obtained for several of the more advanced CD47-targeting agents, including magrolimab, in both preclinical toxicity studies and clinical studies, where anemia and thrombocytopenia were clearly observed.[36 39 66 67]

Collectively, these data show that BYON4228 is a highly differentiating pan-allelic blocking anti-SIRPα antibody, which specifically lacks reactivity with SIRPγ on T cells. In doing so, BYON4228 has the principal features to potentially become a best-in-class drug. Our preclinical functional ADCC and/or ADCP experiments with a variety of target cancer cells and clinically available therapeutic anti-TAAs, including trastuzumab, cetuximab, panitumumab, rituximab and daratumumab, underline the broad potential applicability of BYON4228. This may also extend to other non-anti-TAA combinations, such as other checkpoint inhibitors,[33 34 41 49] chemotherapy[68] and radiotherapy.[35 69] First-in-human clinical studies with BYON4228 are scheduled to start in 2023.

Acknowledgements We thank the Byondis cell line development team and the downstream processing team for generation and purification of critical reagents. We thank Jos van den Crommert, Jenny Vermeer, Tinie van Boekel, Myrthe Rouwette, and Benno Ingelse from Byondis for their assistance with the conception, design and analysis of experiments. We thank Professor Dr I.P. Touw for providing the *Cebpa*$^{Cre/Cre}$ mice.

Contributors MJvH and TKvdB wrote the manuscript with input from all authors. MJvH, SAZ, RJA, HLM, KF, EM-H, DHRFG, DEJWvW, JS, WAK, DvdD, MT, RU, GJAR, GV, MMCvdL, WHAD and TKvdB contributed to the conception and development of the project. SAZ, IMJR-B, MCBCP, LD-E, KdL-A, DD, EWHS-L, DWJvK, IL, HO, HLM, KF, EM-H, MEMS, PJB and BdW performed experiments and analyzed data. DHRFG, DEHWvW, LJ-S and JS generated antibodies (fragments), recombinant proteins and cell lines. RJA, MvdV, JWHS, WAK, DvdD and RU coordinated in vivo studies and (PK) analysis. All authors read and approved the final version of the manuscript. MJvH is responsible for the overall content as guarantor.

Funding The study was sponsored by Byondis BV.

Competing interests TKvdB is inventor on WO 2009/131453; GV, GJAR, RJA, TKvdB, HLM and KF are inventors on WO 2018/210793; GV is inventor on WO 2020/099653.

Patient consent for publication Not applicable.

Ethics approval Not applicable.

Provenance and peer review Not commissioned; externally peer reviewed.

Data availability statement Data are available upon reasonable request.

ORCID iD

Mary J van Helden http://orcid.org/0000-0002-4506-4943

REFERENCES

1 Glennie MJ, van de Winkel JGJ. Renaissance of cancer therapeutic antibodies. *Drug Discov Today* 2003;8:503–10.
2 Strome SE, Sausville EA, Mann D. A mechanistic perspective of monoclonal antibodies in cancer therapy beyond target-related effects. *Oncologist* 2007;12:1084–95.
3 Derer S, Beurskens FJ, Rosner T, *et al*. Complement in antibody-based tumor therapy. *Crit Rev Immunol* 2014;34:199–214.
4 Albanesi M, Mancardi DA, Jönsson F, *et al*. Neutrophils mediate antibody-induced antitumor effects in mice. *Blood* 2013;122:3160–4.
5 Matlung HL, Babes L, Zhao XW, *et al*. Neutrophils kill antibody-opsonized cancer cells by trogoptosis. *Cell Rep* 2018;23:3946–59.
6 Gül N, Babes L, Siegmund K, *et al*. Macrophages eliminate circulating tumor cells after monoclonal antibody therapy. *J Clin Invest* 2014;124:812–23.
7 DiLillo DJ, Ravetch JV. Differential fc-receptor engagement drives an anti-tumor vaccinal effect. *Cell* 2015;161:1035–45.
8 Barclay AN, Van den Berg TK. The interaction between signal regulatory protein alpha (SIRPα) and CD47: structure, function, and therapeutic target. *Annu Rev Immunol* 2014;32:25–50.
9 Matlung HL, Szilagyi K, Barclay NA, *et al*. The CD47-sirpα signaling axis as an innate immune checkpoint in cancer. *Immunol Rev* 2017;276:145–64.
10 Chao MP, Alizadeh AA, Tang C, *et al*. Anti-CD47 antibody synergizes with rituximab to promote phagocytosis and eradicate non-Hodgkin lymphoma. *Cell* 2010;142:699–713.
11 Zhao XW, van Beek EM, Schornagel K, *et al*. CD47-Signal regulatory protein-α (SIRPα) interactions form a barrier for antibody-mediated tumor cell destruction. *Proc Natl Acad Sci U S A* 2011;108:18342–7.
12 Kamber RA, Nishiga Y, Morton B, *et al*. Inter-cellular CRISPR screens reveal regulators of cancer cell phagocytosis. *Nature* 2021;597:549–54.
13 Fujioka Y, Matozaki T, Noguchi T, *et al*. A novel membrane glycoprotein, SHPS-1, that binds the SH2-domain-containing protein tyrosine phosphatase SHP-2 in response to mitogens and cell adhesion. *Mol Cell Biol* 1996;16:6887–99.
14 Adams S, van der Laan LJ, Vernon-Wilson E, *et al*. Signal-regulatory protein is selectively expressed by myeloid and neuronal cells. *J Immunol* 1998;161:1853–9.
15 Veillette A, Thibaudeau E, Latour S. High expression of inhibitory receptor SHPS-1 and its association with protein-tyrosine phosphatase SHP-1 in macrophages. *J Biol Chem* 1998;273:22719–28.
16 Kharitonenkov A, Chen Z, Sures I, *et al*. A family of proteins that inhibit signalling through tyrosine kinase receptors. *Nature* 1997;386:181–6.
17 van Beek EM, Cochrane F, Barclay AN, *et al*. Signal regulatory proteins in the immune system. *J Immunol* 2005;175:7781–7.
18 Jiang P, Lagenaur CF, Narayanan V. Integrin-associated protein is a ligand for the P84 neural adhesion molecule. *J Biol Chem* 1999;274:559–62.
19 Vernon-Wilson EF, Kee WJ, Willis AC, *et al*. CD47 is a ligand for rat macrophage membrane signal regulatory protein SIRP (OX41) and human SIRPalpha 1. *Eur J Immunol* 2000;30:2130–7.
20 Seiffert M, Cant C, Chen Z, *et al*. Human signal-regulatory protein is expressed on normal, but not on subsets of leukemic myeloid cells and mediates cellular adhesion involving its counterreceptor CD47. *Blood* 1999;94:3633–43.
21 Hatherley D, Graham SC, Turner J, *et al*. Paired receptor specificity explained by structures of signal regulatory proteins alone and complexed with CD47. *Mol Cell* 2008;31:266–77.
22 Lindberg FP, Gresham HD, Schwarz E, *et al*. Molecular cloning of integrin-associated protein: an immunoglobulin family member with multiple membrane-spanning domains implicated in alpha v beta 3-dependent ligand binding. *J Cell Biol* 1993;123:485–96.
23 Oldenborg PA, Zheleznyak A, Fang YF, *et al*. Role of CD47 as a marker of self on red blood cells. *Science* 2000;288:2051–4.
24 Abram CL, Roberge GL, Pao LI, *et al*. Distinct roles for neutrophils and dendritic cells in inflammation and autoimmunity in motheaten mice. *Immunity* 2013;38:489–501.
25 Abram CL, Lowell CA. Shp1 function in myeloid cells. *J Leukoc Biol* 2017;102:657–75.
26 Myers DR, Abram CL, Wildes D, *et al*. Shp1 loss enhances macrophage effector function and promotes anti-tumor immunity. *Front Immunol* 2020;11:576310.
27 Chen J, Zhong M-C, Guo H, *et al*. SLAMF7 is critical for phagocytosis of haematopoietic tumour cells via Mac-1 integrin. *Nature* 2017;544:493–7.
28 Veillette A, Chen J. SIRPα-CD47 immune checkpoint blockade in anticancer therapy. *Trends Immunol* 2018;39:173–84.
29 Ring NG, Herndler-Brandstetter D, Weiskopf K, *et al*. Anti-SIRPα antibody immunotherapy enhances neutrophil and macrophage antitumor activity. *Proc Natl Acad Sci USA* 2017;114:E10578–85.
30 Weiskopf K, Ring AM, Ho CCM, *et al*. Engineered SIRPα variants as immunotherapeutic adjuvants to anticancer antibodies. *Science* 2013;341:88–91.
31 Liu X, Pu Y, Cron K, *et al*. CD47 blockade triggers T cell-mediated destruction of immunogenic tumors. *Nat Med* 2015;21:1209–15.
32 Xu MM, Pu Y, Han D, *et al*. Dendritic cells but not macrophages sense tumor mitochondrial DNA for cross-priming through signal regulatory protein α signaling. *Immunity* 2017;47:363–73.
33 Sockolosky JT, Dougan M, Ingram JR, *et al*. Durable antitumor responses to CD47 blockade require adaptive immune stimulation. *Proc Natl Acad Sci USA* 2016;113.
34 Gauttier V, Pengam S, Durand J, *et al*. Selective SIRPα blockade reverses tumor T cell exclusion and overcomes cancer immunotherapy resistance. *J Clin Invest* 2020;130:6109–23.
35 Bian Z, Shi L, Kidder K, *et al*. Intratumoral sirpα-deficient macrophages activate tumor antigen-specific cytotoxic T cells under radiotherapy. *Nat Commun* 2021;12:3229.
36 Advani R, Flinn I, Popplewell L, *et al*. Cd47 blockade by hu5F9-G4 and rituximab in non-Hodgkin's lymphoma. *N Engl J Med* 2018;379:1711–21.
37 Sikic BI, Lakhani N, Patnaik A, *et al*. First-in-human, first-in-class phase I trial of the anti-CD47 antibody hu5f9-G4 in patients with advanced cancers. *J Clin Oncol* 2019;37:946–53.

38 Behrens LM, van den Berg TK, van Egmond M. Targeting the CD47-SIRPα innate immune checkpoint to potentiate antibody therapy in cancer by neutrophils. *Cancers (Basel)* 2022;14:3366.
39 Ansell SM, Maris MB, Lesokhin AM, *et al*. Phase I study of the CD47 blocker TTI-621 in patients with relapsed or refractory hematologic malignancies. *Clin Cancer Res* 2021;27:2190–9.
40 Querfeld C, Thompson JA, Taylor MH, *et al*. Intralesional TTI-621, a novel biologic targeting the innate immune checkpoint CD47, in patients with relapsed or refractory mycosis fungoides or Sézary syndrome: a multicentre, phase 1 study. *Lancet Haematol* 2021;8:e808–17.
41 Lakhani NJ, Chow LQM, Gainor JF, *et al*. Evorpacept alone and in combination with pembrolizumab or trastuzumab in patients with advanced solid tumours (ASPEN-01): a first-in-human, open-label, multicentre, phase 1 dose-escalation and dose-expansion study. *Lancet Oncol* 2021;22:1740–51.
42 Brown EJ, Frazier WA. Integrin-associated protein (CD47) and its ligands. *Trends Cell Biol* 2001;11:130–5.
43 Kaur S, Martin-Manso G, Pendrak ML, *et al*. Thrombospondin-1 inhibits VEGF receptor-2 signaling by disrupting its association with CD47. *J Biol Chem* 2010;285:38923–32.
44 Soto-Pantoja DR, Stein EV, Rogers NM, *et al*. Therapeutic opportunities for targeting the ubiquitous cell surface receptor CD47. *Expert Opin Ther Targets* 2013;17:89–103.
45 Brooke G, Holbrook JD, Brown MH, *et al*. Human lymphocytes interact directly with CD47 through a novel member of the signal regulatory protein (SIRP) family. *J Immunol* 2004;173:2562–70.
46 Stefanidakis M, Newton G, Lee WY, *et al*. Endothelial CD47 interaction with sirpgamma is required for human T-cell transendothelial migration under shear flow conditions in vitro. *Blood* 2008;112:1280–9.
47 Piccio L, Vermi W, Boles KS, *et al*. Adhesion of human T cells to antigen-presenting cells through sirpbeta2-CD47 interaction costimulates T-cell proliferation. *Blood* 2005;105:2421–7.
48 Dehmani S, Nerrière-Daguin V, Néel M, *et al*. SIRPγ-CD47 interaction positively regulates the activation of human T cells in situation of chronic stimulation. *Front Immunol* 2021;12:732530.
49 Liu J, Xavy S, Mihardja S, *et al*. Targeting macrophage checkpoint inhibitor SIRPα for anticancer therapy. *JCI Insight* 2020;5:e134728.
50 Sim J, Sockolosky JT, Sangalang E, *et al*. Discovery of high affinity, pan-allelic, and pan-mammalian reactive antibodies against the myeloid checkpoint receptor SIRPα. *MAbs* 2019;11:1036–52.
51 Voets E, Paradé M, Lutje Hulsik D, *et al*. Functional characterization of the selective pan-allele anti-SIRPα antibody ADU-1805 that blocks the sirpα-CD47 innate immune checkpoint. *J Immunother Cancer* 2019;7:340.
52 Wu Z-H, Li N, Mei X-F, *et al*. Preclinical characterization of the novel anti-sirpα antibody BR105 that targets the myeloid immune checkpoint. *J Immunother Cancer* 2022;10:e004054.
53 Andrejeva G, Capoccia BJ, Hiebsch RR, *et al*. Novel SIRPα antibodies that induce single-agent phagocytosis of tumor cells while preserving T cells. *J Immunol* 2021;206:712–21.
54 Poirier NM, Van-Hove B, Gauttier V, *et al*. OSE immunotherapeutics, assignee. new anti-sirpa antibodies and their therapeutic applications. 2017.
55 Kuo TC, Chen A, Harrabi O, *et al*. Targeting the myeloid checkpoint receptor SIRPα potentiates innate and adaptive immune responses to promote anti-tumor activity. *J Hematol Oncol* 2020;13:160.
56 Hatherley D, Lea SM, Johnson S, *et al*. Polymorphisms in the human inhibitory signal-regulatory protein α do not affect binding to its ligand CD47. *J Biol Chem* 2014;289:10024–8.
57 Seiffert M, Brossart P, Cant C, *et al*. Signal-Regulatory protein alpha (SIRPalpha) but not SIRPbeta is involved in T-cell activation, binds to CD47 with high affinity, and is expressed on immature CD34 (+) CD38 (-) hematopoietic cells. *Blood* 2001;97:2741–9.
58 Abbasian MC, Escoubet L, Fenalti G, *et al*. SIRPα binding proteins and methods of use thereof. 2020.
59 Kurlander RJ. Blockade of Fc receptor-mediated binding to U-937 cells by murine monoclonal antibodies directed against a variety of surface antigens. *J Immunol* 1983;131:140–7.
60 Koentgen F, Lin J, Katidou M, *et al*. Exclusive transmission of the embryonic stem cell-derived genome through the mouse germline. *Genesis* 2016;54:326–33.
61 Murata Y, Tanaka D, Hazama D, *et al*. Anti-Human SIRPα antibody is a new tool for cancer immunotherapy. *Cancer Sci* 2018;109:1300–8.
62 Leabman MK, Meng YG, Kelley RF, *et al*. Effects of altered FcγR binding on antibody pharmacokinetics in cynomolgus monkeys. *MAbs* 2013;5:896–903.
63 Hezareh M, Hessell AJ, Jensen RC, *et al*. Effector function activities of a panel of mutants of a broadly neutralizing antibody against human immunodeficiency virus type 1. *J Virol* 2001;75:12161–8.
64 Strati P, Hawkes E, Ghosh N, *et al*. Interim results from the first clinical study of CC-95251, an anti-signal regulatory protein-alpha (SIRPα) antibody, in combination with rituximab in patients with relapsed and/or refractory non-hodgkin lymphoma (R/R NHL). *Blood* 2021;138:2493.
65 Hogarth PM, Pietersz GA. Fc receptor-targeted therapies for the treatment of inflammation, cancer and beyond. *Nat Rev Drug Discov* 2012;11:311–31.
66 Liu J, Wang L, Zhao F, *et al*. Pre-clinical development of a humanized anti-CD47 antibody with anti-cancer therapeutic potential. *PLoS One* 2015;10:e0137345.
67 Petrova PS, Viller NN, Wong M, *et al*. TTI-621 (sirpαfc): a CD47-blocking innate immune checkpoint inhibitor with broad antitumor activity and minimal erythrocyte binding. *Clin Cancer Res* 2017;23:1068–79.
68 Wang C, Sallman DA. Targeting the cluster of differentiation 47/signal-regulatory protein alpha axis in myeloid malignancies. *Curr Opin Hematol* 2022;29:44–52.
69 Hsieh RC-E, Krishnan S, Wu R-C, *et al*. Atr-Mediated CD47 and PD-L1 up-regulation restricts radiotherapy-induced immune priming and abscopal responses in colorectal cancer. *Sci Immunol* 2022;7:eabl9330.
70 Poirier N, Gauttier V, Mary C, *et al*. Use of anti-human SIRPA V1 antibodies and method for producing anti-SIRPA V1 antibodies. 2019.
71 Events and presentations. n.d. Available: https://ir.fortyseveninc.com/events-and-presentations
72 Treffers LW, van Houdt M, Bruggeman CW, *et al*. FcγRIIIb restricts antibody-dependent destruction of cancer cells by human neutrophils. *Front Immunol* 2018;9:3124.